ACCOUNTS
of chemical research

Theoretical and Experimental Insights into the Origin of the Catalytic Activity of Subnanometric Gold Clusters: Attempts to Predict Reactivity with Clusters and Nanoparticles of Gold

MERCEDES BORONAT, ANTONIO LEYVA-PÉREZ, AND AVELINO CORMA*

Instituto de Tecnología Química, Universidad Politécnica de Valencia − Consejo Superior de Investigaciones Científicas, Av. los Naranjos, s/n, 46022 Valencia, Spain

RECEIVED ON MARCH 7, 2013

CONSPECTUS

Particle size is one of the key parameters determining the unexpected catalytic activity of gold, with reactivity improving as the particle gets smaller. While this is valid in the 1−5 nm range, chemists are now investigating the influence of particle size in the subnanometer regime. This is due to recent advances in both characterization techniques and synthetic routes capable of stabilizing these size-controlled gold clusters. Researchers reported in early studies that small clusters or aggregates of a few atoms can be extremely active in some reactions, while 1−2 nm nanoparticles are catalytically more efficient for other reactions. Furthermore, the possibility that small gold clusters generated in situ from gold salts or complexes could be the real active species in homogeneous gold-catalyzed organic reactions should be considered.

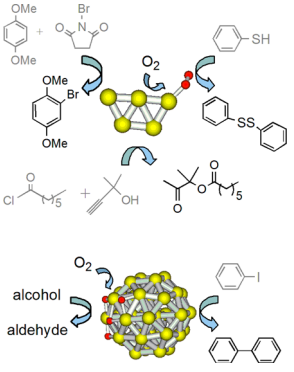

In this Account, we address two questions. First, what is the origin of the enhanced reactivity of gold clusters on the subnanometer scale? And second, how can we predict the reactions where small clusters should work better than larger nanoparticles? Both geometric factors and electronic or quantum size effects become important in the subnanometer regime. Geometric reasons play a key role in hydrogenation reactions, where only accessible low coordinated neutral Au atoms are needed to dissociate H_2. The quantum size effects of gold clusters are important as well, as clusters formed by only a few atoms have discrete molecule-like electronic states and their chemical reactivity is related to interactions between the cluster's frontier molecular orbitals and those of the reactant molecules.

From first principles calculations, we predict an enhanced reactivity of small planar clusters for reactions involving activation of CC multiple bonds in alkenes and alkynes through Lewis acid−base interactions, and a better catalytic performance of 3D gold nanoparticles in redox reactions involving bond dissociation by oxidative addition and new bond formation by reductive elimination. In oxidation reactions with molecular O_2, initial dissociation of O_2 into basic oxygen atoms would be more effectively catalyzed by gold nanoparticles of ∼1 nm diameter. In contrast, small planar clusters should be more active for reactions following a radical pathway involving peroxo or hydroperoxo intermediates. We have experimentally confirmed these predictions for a series of Lewis acid and oxidation reactions catalyzed by gold clusters and nanoparticles either in solution or supported on solid carriers.

Introduction

Gold has attracted wide interest as a catalyst in the last 25 years due to its unexpected activity under mild temperature and pressure conditions. Small gold nanoparticles finely dispersed on solid supports are active and highly selective in a large number of organic reactions.[1−4] The catalytic activity of gold depends on some key parameters, such as particle size and shape, interaction with the support, oxidation state, and quantum size effects.[5,6] However, these parameters are not completely independent. As particle size decreases, the number of atoms accessible to reactants, as well as the relative concentration of the more reactive low coordinated atoms at corner or edge positions, increase. Moreover, the number of gold atoms in direct contact with the support varies with particle diameter and shape, which might lead to enhanced reactivity when gold nanoparticles are supported on noninert metal oxides.

Published on the Web 06/10/2013 www.pubs.acs.org/accounts
10.1021/ar400068w

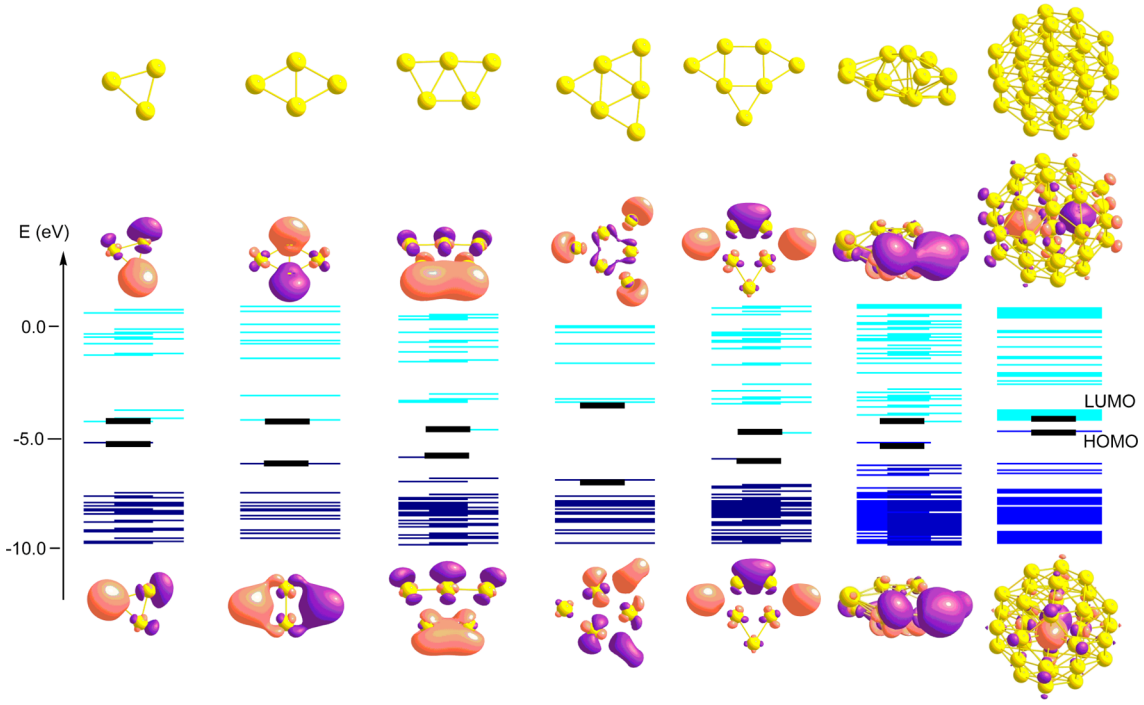

FIGURE 1. Optimized structure (top) and calculated isosurfaces of the lowest unoccupied molecular orbital (LUMO, center) and highest occupied molecular orbital (HOMO, bottom) of Au_3, Au_4, Au_5, Au_6, Au_7, Au_{13}, and Au_{38} clusters, together with molecular orbital energy levels in blue. Obtained at the B3LYP/LANL2DZ level using the Gaussian09 program.

In agreement with these arguments, Haruta et al. reported that the activity for CO oxidation of gold nanoparticles supported on TiO_2, α-Fe_2O_3, and Co_3O_4 increases sharply when particle diameter goes below 4 nm,[7] and a similar behavior was reported for the aerobic oxidation of alcohols over Au/TiO_2[8] and with PVP-stabilized gold clusters.[9] On the other hand, a volcano type curve with a maximum in activity at a gold particle diameter of ~3 nm was reported for CO oxidation over Au/TiO_2 catalysts[10] and for aerobic alcohol oxidation over Au/MgO,[11] showing that particle morphology is another critical parameter for catalytic activity. It has also been demonstrated that the most active sites for different reactions are not necessarily the same, and that the optimum particle size for a given reaction depends on the material used as support.[12−15]

While the key role of gold particle size is clear, the study of the subnanometric regime is a challenging task due to the difficulty to obtain a homogeneous distribution of cluster sizes and due to technical limitations to characterize aggregates of few gold atoms. However, the stabilization of size-controlled gold clusters either in solution or supported on solids and recent advances in characterization techniques have allowed identification of subnanometric gold nanoparticles in different materials.[16] Concerning catalysis, bilayer clusters of ~0.5 nm in diameter have been identified as the active species for CO oxidation over Au/FeO_x catalysts,[17] and Au_6−Au_{10} clusters supported on Al_2O_3 films are active for propene epoxidation.[18] Nevertheless, the reactivity of small gold clusters is not limited to oxidation reactions, and it has been recently demonstrated that small Au_3 clusters in gas phase are able to dissociate the C−I bond in iodobenzene while mononuclear Au^+ cations are not.[19]

It is interesting to notice that, in many organic reactions, gold salts and gold complexes are claimed as active catalysts, though the starting gold species may decompose during reaction.[20−22] In these cases in which the catalyst introduced in the reaction media is not the true active species, but this is formed in the course of the reaction, an induction period should be observed provided that the rates of catalyst formation and reaction are decoupled. At this point, our starting hypothesis was that small clusters generated in situ from gold salts or complexes might be the real active species in a number of homogeneous gold-catalyzed organic reactions. A specific experimental program was then undertaken to study the additional possibilities that gold clusters can offer with respect to gold nanoparticles. Simultaneously we investigated how the geometric and electronic differences between gold clusters and nanoparticles can determine their activity and selectivity. We expected that,

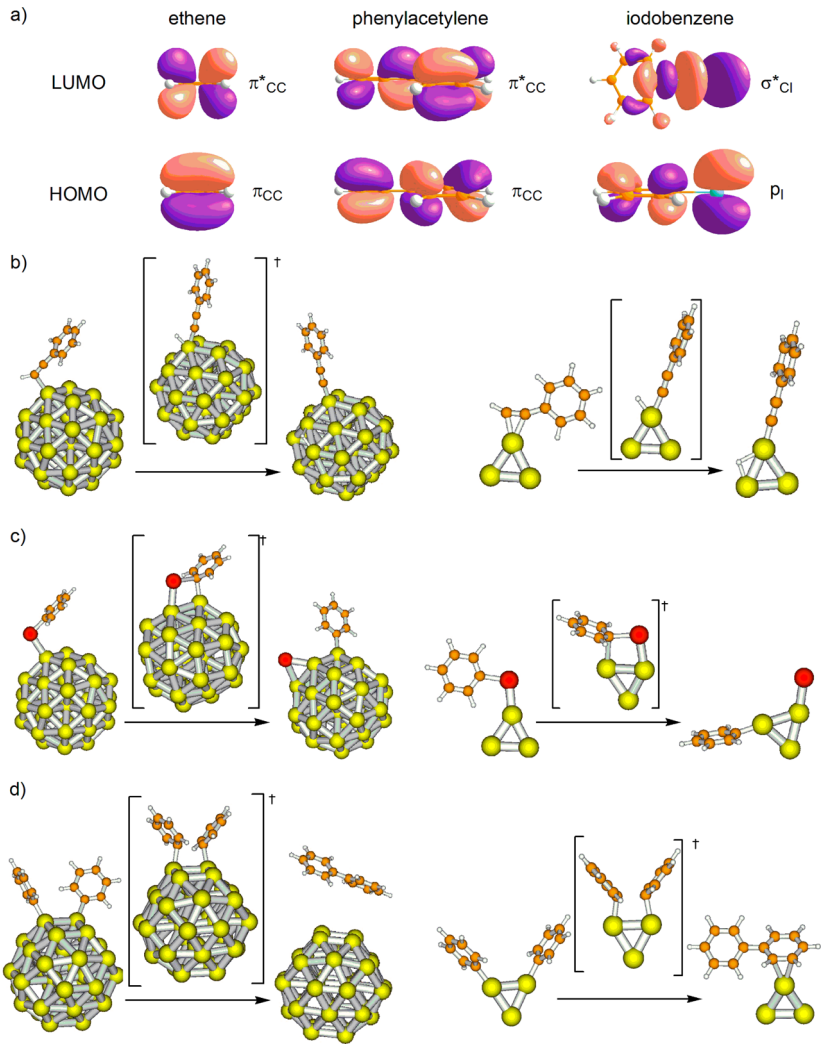

FIGURE 2. Frontier orbitals of ethene, phenylacetylene, and iodobenzene (a). Optimized structures involved in phenylacetylene deprotonation (b), iodobenzene dissociation (c), and coupling step (d) over a Au_{38} nanoparticle and a Au_3 cluster. Au, O, C, and H atoms are depicted in yellow, red, orange, and white, respectively.

based on this, it would be possible to predict the suitability of each type of gold catalysts for a given reaction.

Geometric and Electronic Differences between Au Clusters and Nanoparticles

Due to strong relativistic effects in gold that induce hybridization of the atomic 5*d*-6*s* orbitals, two-dimensional structures are the most stable configuration of gold clusters formed by up to 7 atoms (Figure 1).[23] The frontier orbitals of planar Au_N clusters consist of several lobes localized on the low coordinated Au atoms and fully accessible to interaction with reactant molecules. However, when particle morphology changes from planar to 3D and the coordination number of the surface atoms increases, the contribution of the atoms inside the particle to the composition of the frontier orbitals becomes more important, and therefore orbital overlap with interacting molecules would be less efficient.

On the other hand, the discrete electronic levels in the smallest Au_N clusters are more separated than in larger nanoparticles,[24] and the number of electrons energetically accessible to be transferred to reactant molecules in redox processes increases with increasing number of gold atoms in the system. So, depending on the type of interaction involved in the catalytic process, a different molecular interaction and reactivity could be expected for small planar clusters and larger 3D nanoparticles.

Interaction of Molecules with Au Clusters and Nanoparticles

Gold as Lewis Acid Catalyst. When gold acts as Lewis acid, molecular binding involves electron density transfer

TABLE 1. Interaction of Different Molecules with Au_3 Cluster and Au_{38} Nanoparticle[a]

	Au_3			Au_{38}			gas
	E_{int} (kcal/mol)[b]	Δq (e)[c]	r_{XY} (Å)[d]	E_{int} (kcal/mol)[b]	Δq (e)[c]	r_{XY} (Å)[d]	r_{XY} (Å)[d]
propene	−37.8	−0.11	1.41	−12.3	−0.16	1.38	1.33
phenylacetylene	−37.0	−0.06	1.26	−11.9	−0.15	1.25	1.21
H_2O	−15.5	−0.11	0.97	−5.4	−0.07	0.97	0.97
ethanol	−18.3	−0.13	0.97	−9.1	−0.08	0.97	0.97
thiophenol	−32.6	−0.24	1.36	−13.2	−0.20	1.35	1.35
iodobenzene	−28.3	−0.28	2.15	−16.6	−0.26	2.12	2.13
O_2 (top)	−22.0	0.36	1.29				1.25
O_2 (bridge)	−23.0	0.40	1.32	−22.8	0.62	1.37	1.25
O_2 (bb)				−22.6	0.87	1.46	1.25

[a]Calculated using the VASP code, PW91 functional, and plane wave basis set with a cutoff of 500 eV and PAW potential. All systems were placed in a $20 \times 20 \times 20$ Å^3 cubic box, and calculations were carried out at the Γ k-point of the Brillouin zone. [b]Calculated as $E_{int} = E(Au_N\text{-adsorbate}) - E(Au_N) - E(\text{adsorbate})$. [c]Net charge transferred to Au_N upon molecular adsorption obtained from Bader AIM analysis. Negative values imply electron density from molecule to gold. [d]r_{XY} corresponds to r_{CC} in propene and phenylacetylene, r_{OH} in H_2O and ethanol, r_{SH} in thiophenol, r_{CI} in iodobenzene, and r_{OO} in O_2.

from the highest occupied molecular orbital (HOMO) of the adsorbing molecule to the lowest unoccupied molecular orbital (LUMO) of the cluster. The binding of Lewis bases such as alkenes and alkynes involves charge transfer from the occupied π CC orbital of the multiple CC bond to the LUMO of the cluster, and back-donation from gold to the π^* (CC) orbital of the corresponding alkene or alkyne (Figure 2a). These two charge transfer processes produce an activation and weakening of the multiple CC bond that is reflected in an elongation of the CC distances (Table 1). The more efficient orbital overlap achieved on small planar clusters leads to a larger interaction energy and also to a higher degree of CC bond activation, that should cause a higher reactivity. Indeed, the activation energy for deprotonation of phenylacetylene yielding a σ-bonded complex is considerably lower on an Au_3 cluster (30 kcal/mol) than over a Au_{38} nanoparticle (40 kcal/mol).

The HOMO of other Lewis bases such as water, alcohols, and thiols is localized on the corresponding *p* orbitals on O and S atoms, and the spatial overlap with the protruding lobe of the LUMO on an isolated Au_3 cluster is considerably more efficient than with the LUMO on a Au_{38} nanoparticle. There is a clear correlation between the degree of charge transfer and the calculated interaction energy (Table 1), but this interaction does not lead to any activation of the O−H or S−H bonds, and therefore an enhanced reactivity on smaller clusters cannot be inferred in this case.

Gold as Redox Catalyst. Coupling reactions between aryl halides, arylboronic acids, and alkenes or alkynes resulting in formation of new C−C bonds are also catalyzed by gold.[25−27] These reactions usually involve some bond dissociation by oxidative addition and new bond formation by reductive elimination. Aryl halides such as iodobenzene bind to gold by electron density transfer from the lone pair on the halide

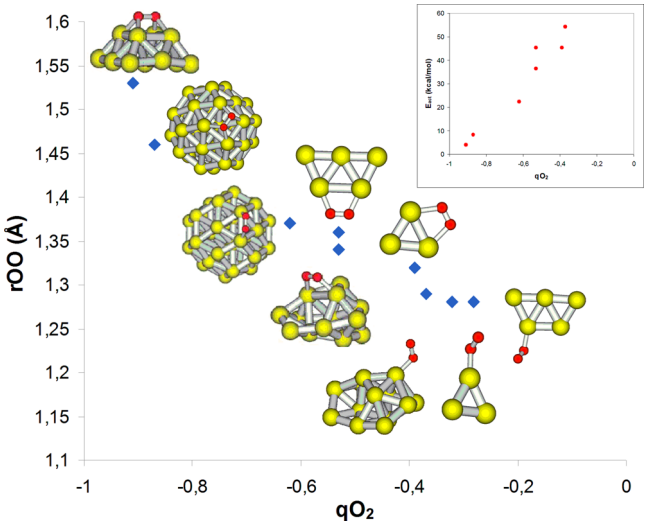

FIGURE 3. Optimized structures of O_2 interacting with Au_{38}, Au_{13}, Au_5, and Au_3 clusters, and correlation between optimized OO bond length and charge transferred to O_2. Inset: correlation between activation barrier for O_2 dissociation and charge transferred to O_2.

atom to the LUMO of the cluster, and the C−I bond is activated by back-donation from gold to the antibonding σ_{CI} molecular orbital. Binding of iodobenzene to either Au_3 or Au_{38} systems stabilizes the σ_{CI} molecular orbital by ∼1 eV with respect to gas phase molecule, facilitating in both cases charge transfer and bond activation. The better accessibility of the electrons in the discrete electronic levels of larger nanoparticles facilitates this process, and consequently the activation barrier for iodobenzene dissociation on a Au_{38} nanoparticle is lower than that on a Au_3 cluster, 11.3 and 15.8 kcal/mol, respectively. The resulting phenyl fragments are more stabilized on the less coordinated Au_3 clusters, and as a consequence the activation barrier for the C−C coupling step is ∼4 kcal/mol larger on Au_3 than on Au_{38} (Figure 2). These values suggest that gold nanoparticles of ∼1 nm

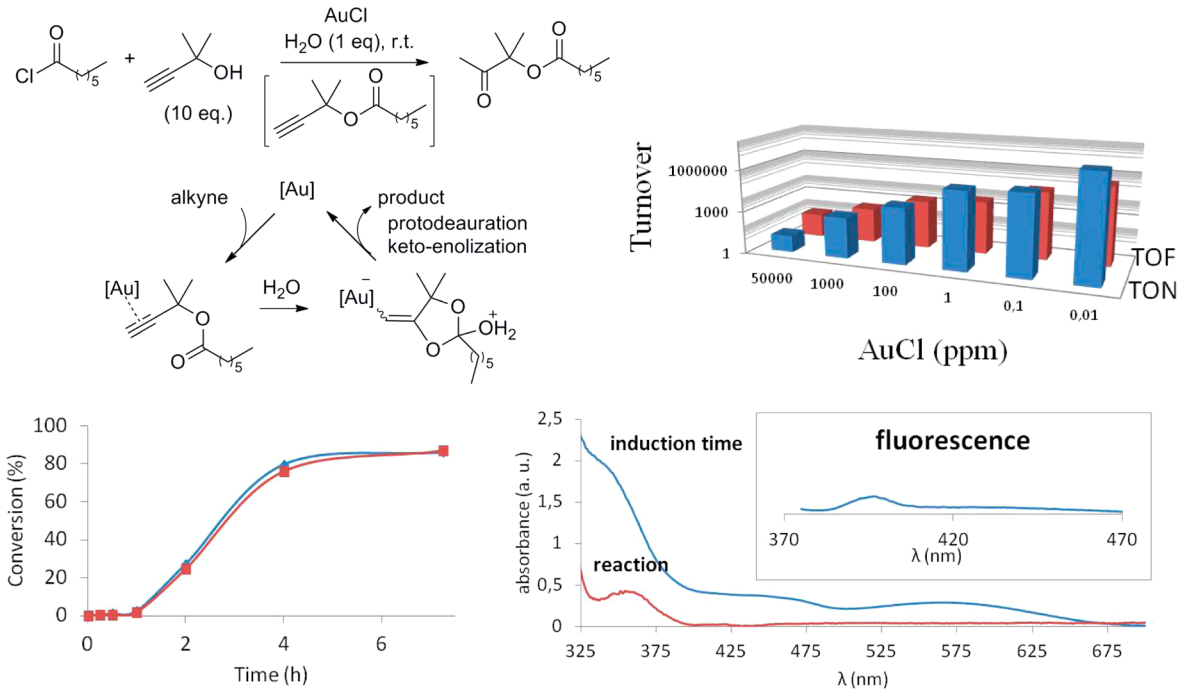

FIGURE 4. (a) Reaction scheme and possible mechanism for ester-assisted hydration of alkynes. (b) Turnover number (TON) and turnover frequency (TOF) for different amounts of AuCl. (c) Plot-time conversion for AuCl (squares) and $HAuCl_4$ (diamonds) at 100 ppm. (d) Absorption measurements (a.u., arbitrary units) for the hydration reaction containing the Au active species during the induction time and when the reaction proceeds. Inset: corresponding fluorescence, irradiated at 349 nm.

diameter could be more active than small planar clusters for coupling reactions.

Gold as Oxidation Catalyst with O_2. The interaction of molecular O_2 with gold, which is a key step in gold-catalyzed oxidation reactions, involves electron density transfer from the metal to the empty π^* (OO) molecular orbital of O_2.[28] The degree of charge transfer and therefore of molecular activation depends on the spatial overlap between the HOMO of the gold cluster and the π^* orbital of O_2, and this is related to the mode of adsorption of O_2 on gold (Figure 3). The largest degree of charge transfer and therefore of OO bond activation is found in bridge−bridge complexes (*bb*), in which each oxygen atom in O_2 is bonded to two Au atoms, and the four Au atoms involved are arranged as in the Au(100) facet. The *bridge* conformation, in which O_2 lies parallel to an Au−Au bond and each oxygen atom in O_2 is directly bonded to one Au atom, produces an intermediate degree of molecular activation or peroxo species, and adsorption in an end-on or *top* mode in which O_2 is almost perpendicular to the gold surface and only one oxygen atom is directly bonded to a low coordinated Au atom leads to a weaker molecular activation or superoxo species.[29,30] A previous theoretical study in our group concluded that O_2 adsorption and dissociation into adsorbed oxygen atoms are structure-sensitive processes, that mainly depend on particle morphology.[29] When gold particle size goes below ∼0.5 nm, the irregular and/or planar shape of the clusters does not allow the presence of (100) facets that stabilize the *bb* conformation, and therefore only *bridge* and *top* conformations exist, for which the calculated O_2 dissociation activation energies are considerably larger (Figure 3, inset).[29,31] The ability of Au NPs of ∼1 nm diameter to dissociate O_2 was experimentally confirmed, and both chemisorbed oxygen atoms and oxide-like structures composed by linear O−Au−O units were theoretically and experimentally identified.[32,33]

These results indicate that, in principle, chemisorbed oxygen atoms and oxide-like O−Au−O structures should be present on 3D gold clusters of ∼1 nm diameter, while molecularly adsorbed superoxo species and, depending on reaction conditions, hydroperoxide −OOH groups[18,34] would be the active oxygen species on planar gold clusters of low atomicity.

Testing Reactivity Predictions by Experimental Catalytic Results

From the above considerations, we predicted an enhanced reactivity of small planar Au_N clusters for reactions involving activation of the CC multiple bond in alkenes and alkynes, while redox reactions involving bond dissociation by oxidative addition and new bond formation by reductive

elimination should be more efficiently catalyzed by 3D gold nanoparticles. In the case of oxidation reactions with molecular O_2, for those processes requiring the participation of basic O^- species, 3D gold nanoparticles should be more active than clusters, while for mechanisms involving radical species, small planar gold clusters would be the preferred catalyst.

Lewis Acid Catalysis with Au Clusters. We have recently reported[35] that gold clusters of 3−5 atoms catalyze the ester-assisted hydration of alkynes in solution with millions of turnovers at room temperature. When the reaction kinetics were studied in the presence of large amounts of gold salts (~5 mol %) no induction period was apparent, but when the reaction was carried out in the presence of only 100 ppm of either AuCl or $HAuCl_4$, an induction period of 1 h was observed, after which the reaction proceeded with the same rate regardless the starting salt used (Figure 4). These results suggest that neither AuCl nor $HAuCl_4$ is the active species, but others formed from the gold salts during the induction period. The evolution of gold species was followed by MALDI-TOF spectrometry and UV−vis spectroscopy, and it was found that the reaction started only when Au_3−Au_5 clusters predominated, indicating that these are indeed the true active species. To further confirm this conclusion, Au_5 and Au_8 clusters stabilized on the dendrimer poly(amineamide−ethanol) (PAMAM−OH) were independently synthesized,[36] and Figure 5 shows that while Au_5−PAMAM catalyzed the reaction at ppm concentrations, Au_8−PAMAM did not.

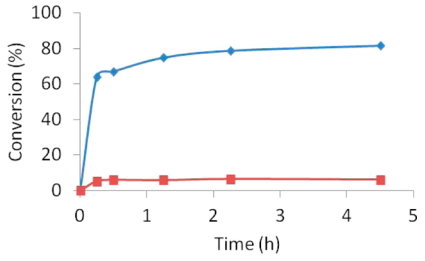

FIGURE 5. Plot-time conversion for the ester assisted hydration of alkynes with Au_5−PAMAM (◇) and Au_8−PAMAM (□).

The selective bromination of arenes with *N*-bromosuccinimide is catalyzed by $AuCl_3$,[37] and activity was attributed to the high Lewis acidity of Au^{III}. If this was so, less acidic AuCl should work poorly as catalyst. However, when the bromination of *p*-dimethoxybenzene was performed with catalytic amounts of AuCl or $AuCl_3$, an induction period was observed after which a similar activity was observed regardless the initial gold salt used (Figure 6). Gold clusters of 7−9 atoms were identified by UV−vis measurements as responsible for the catalysis. In accordance, the performance of Au_8−PAMAM was better than that of Au_5−PAMAM, while gold nanoparticles were not active for this reaction, as predicted above.

To further confirm that different reactions are catalyzed by different gold clusters, the reactants of the two Lewis acid reactions considered were mixed in a single vessel and then AuCl was added. UV−vis and MALDI-TOF studies during the ester-assisted hydration of alkynes had shown that the initial gold species formed from AuCl are predominantly clusters of 6−9 atoms and, in accordance, the bromination of *p*-dimethoxybenzene proceeded from the beginning. However, after the expected induction time, 3−5 atom gold clusters take over and the hydration proceeds while the

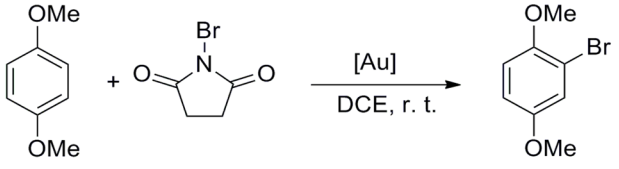

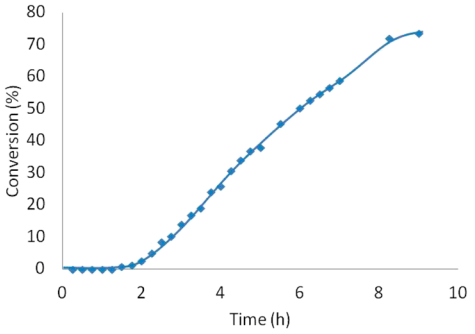

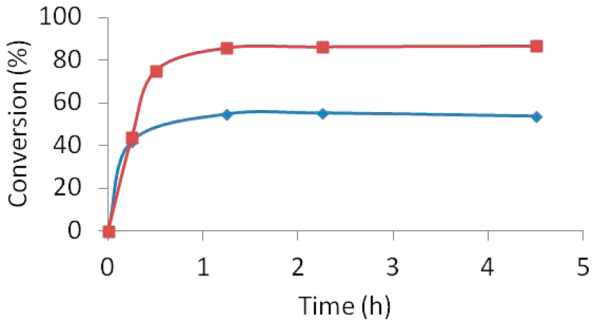

FIGURE 6. Plot-time conversion for the gold-catalyzed bromination of arenes. Left: with 100 ppm of AuCl. Right: with Au_8−PAMAM (□) and Au_5−PAMAM (◇).

TABLE 2. Iodobenzene Homocoupling Catalyzed by Gold Nanoparticles and Clusters

gold catalyst	conversion (%)[a]
Au/TiO_2	100
AuCl + butynol + HCl	<5
Au_5−PAMAM	18

[a]Measured by GC. Biphenyl was the only product found.

bromination stops. In other words, each reaction proceeds independently depending on the type of gold cluster present in solution.

Redox Catalysis with Au Nanoparticles: Homocoupling of Iodobenzene. The homocoupling of iodobenzene has been reported on gold nanoparticles[20−22] and extended surfaces.[38] The reaction mechanism involves initial dissociation of the C−I bond by oxidative addition and subsequent formation of the new C−C bond between two phenyl fragments by reductive elimination (Figure 2c,d), and, according to the DFT calculations previously described, 3D gold nanoparticles should be more active than planar Au_3 clusters for coupling reactions. To experimentally confirm whether iodobenzene homocoupling occurs on gold nanoparticles or clusters, we used commercial Au/TiO_2 containing metallic nanoparticles of 3.0 ± 0.5 nm, gold clusters generated in situ, and Au_5−PAMAM. Table 2 shows that while Au/TiO_2 catalyzes iodobenzene homocoupling quantitatively, in situ generated gold clusters and Au_5−PAMAM give very low conversions, demonstrating that iodobenzene homocoupling preferentially occurs on gold nanoparticles.

Activation of Molecular Oxygen on Gold Nanoparticles: Formation of Chemisorbed O Atoms as Active Species. The mechanism of gold-catalyzed alcohol oxidation involves an initial deprotonation of the hydroxyl group forming a metal-alkoxide intermediate that, in a second step, suffers a β-hydride elimination yielding the carbonylic product, while O_2 reacts with the abstracted H atoms to produce H_2O (Figure 7a) or participates in the first step of the mechanism by assisting in the deprotonation of the alcohol (Figure 7b). When gold nanoparticles are supported on metal oxides, the alkoxide intermediate is probably formed on the support or at the metal−support interface. But when the reaction is catalyzed by naked gold nanoparticles in solution, stabilized by polymers, or supported on carbon or SiO_2, activity has been related to the presence of low coordinated atoms

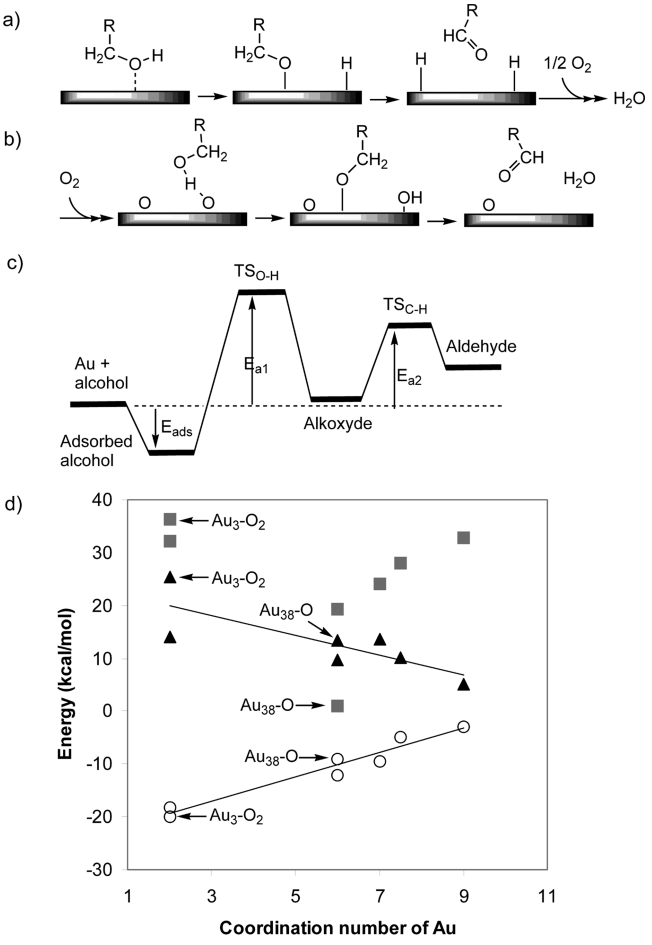

FIGURE 7. Reaction mechanism of gold-catalyzed alcohol oxidation to aldehydes with (a) oxygen removing adsorbed H atoms after reaction or (b) oxygen directly participating in alcohol deprotonation. (c) Energy profile. (d) Plot of calculated adsorption energies (E_{ads}, empty circles), activation energies for OH dissociation (E_{aOH}, gray squares), and for C−H_β bond scission (E_{aCH}, black triangles) versus coordination number of gold. Arrows point to the values corresponding to systems with adsorbed O atoms (over Au_{38} nanoparticles, coordination number 6) or O_2 molecule (over Au_3 cluster, coordination number 2). Adsorption energies have been calculated as $E_{ads} = E$(adsorption complex) − E(ethanol) − E(catalyst), where the term catalyst includes the gold cluster or nanoparticle and adsorbed oxygen species if present.

placed at corner or edge positions,[8,39−41] and indeed, a direct relationship between activation barriers and coordination number of Au atoms was theoretically obtained (Figure 7c,d).[11] However, the effect of chemisorbed basic O atoms is considerably more important and decreases the activation energy for deprotonation of the hydroxyl group by ∼20 kcal/mol (Figures 7d, 8), while it has no influence on the dissociation of the C−H_β bond.[42] The reaction path for ethanol oxidation over a Au_3 cluster has been here investigated, and although the interaction of ethanol with the low coordinated atoms in Au_3 is considerably stronger than that with the Au_{38} nanoparticle, the activation energy

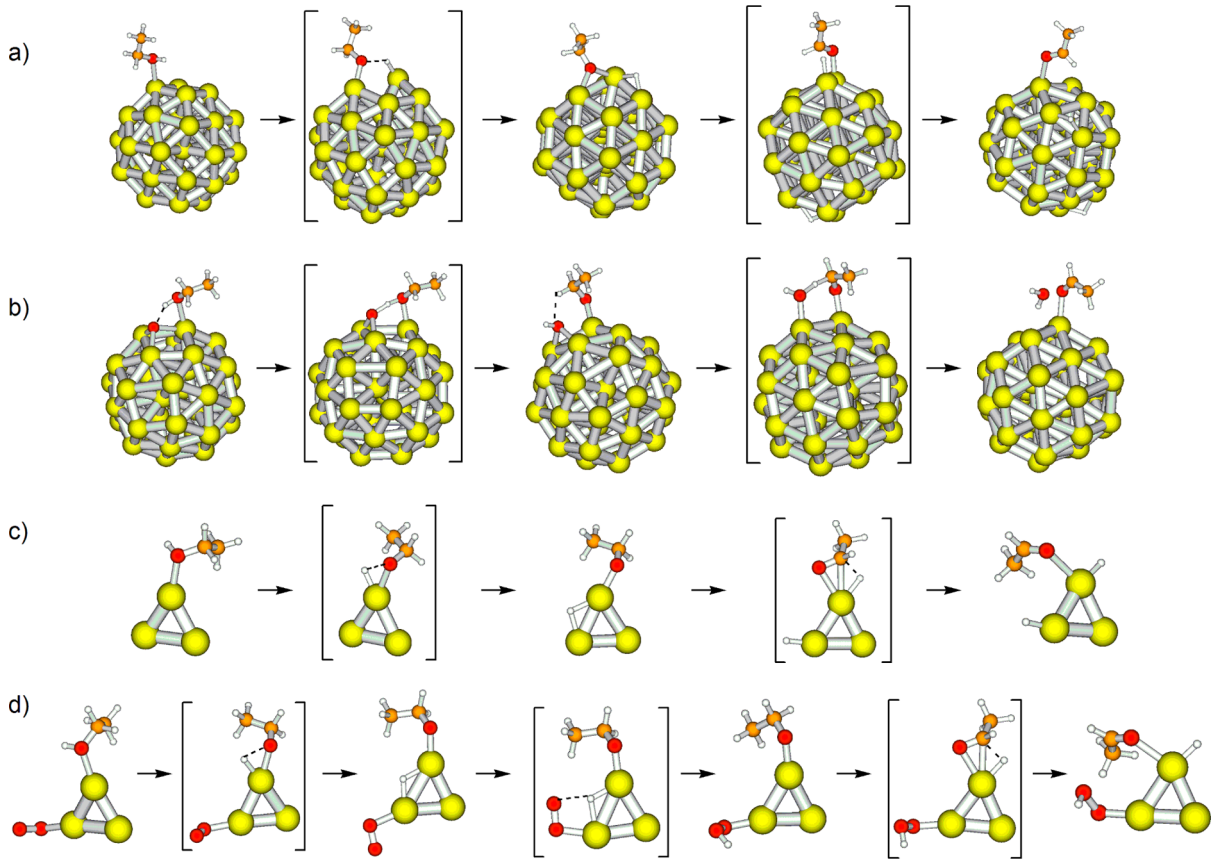

FIGURE 8. Structures involved in gold-catalyzed alcohol oxidation. The catalyst model is (a) Au_{38} nanoparticle, (b) Au_{38} nanoparticle with chemisorbed O, (c) Au_3 cluster, and (d) Au_3 cluster with adsorbed O_2. Au, O, C, and H atoms are depicted in yellow, red, orange, and white, respectively.

for deprotonation is ~10 kcal/mol larger (Figure 7d). The presence of coadsorbed activated O_2 does not assist in this process since, as shown in Figure 8d, the proton of ethanol hydroxyl group is not directly transferred to adsorbed O_2, but to the gold cluster with an activation barrier as high as 36 kcal/mol. It can then be concluded that alcohol oxidation is very favored by the presence of chemisorbed oxygen atoms able to abstract protons and dissociate the hydroxyl group. These basic oxygen atoms are stabilized on 3D gold nanoparticles and not on small planar clusters. In agreement with these theoretical predictions, experimental tests with in situ generated gold clusters in solution under aerobic conditions did not show significant oxidation conversion for different alcohols, in contrast to the previously reported activity of gold nanoparticles for alcohol oxidation to aldehydes or acids.[8,9,11,37−39]

Activation of Molecular Oxygen on Gold Clusters: Formation of Radical Peroxides as Active Species. Recent work in our group has shown that Au/CeO_2 catalyzes the oxidation of thiols to disulfides with oxygen, in absence of solvent or in aqueous media at room temperature.[43] A radical pathway was proposed for this reaction, according to which the thiol SH bond dissociates homolytically into a H atom and a thiyl radical that forms an Au-thiolate species. O_2 acts as the final electron acceptor, reacting with the H atoms to form either H_2O or H_2O_2.

$$2RSH + \frac{1}{2}O_2 \rightarrow 2RSSR + H_2O$$

Taking into account the frontier orbital arguments discussed before, radical mechanisms should be favored over small isolated gold clusters. To identify the active species for disulfide formation, isolated gold atoms, gold clusters with 5−10 atoms, and gold nanoparticles of ~1 nm were supported on carbon nanotubes and their activity in the oxidation of thiophenol tested (Figure 9).[44] Gold species were characterized by HAADF-STEM, XAS, and UV−vis spectroscopies, and it was found that only clusters with 5−10 atoms were active for this reaction, in agreement with the theoretical prediction that small planar clusters should be more active than nanoparticles in oxidation reactions involving radical peroxo

or hydroperoxo intermediates. The complete reaction path for thiol oxidation over isolated Au^I species, Au_5 clusters, and Au_{38} nanoparticles was investigated by means of DFT calculations (Figure 10), and both the initial induction period observed when using isolated atoms as catalyst and the decrease in activity observed with increasing particle size were explained in terms of ability to activate molecular O_2 and catalyst poisoning by formation of very stable linear RS-Au-SR units on 3D nanoparticles.[45,46]

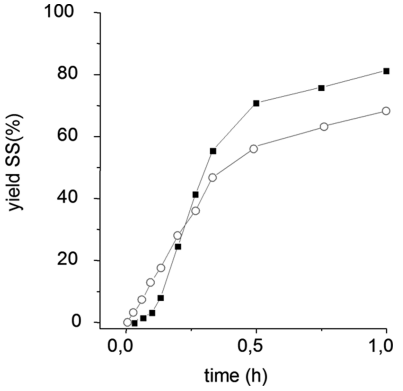

FIGURE 9. Yield to disulfide with reaction time over gold atoms (■) and over gold clusters (○). Gold nanoparticles are inactive.

Conclusions

The geometric and electronic differences between gold clusters comprising a few atoms and gold nanoparticles of 1 nm or larger determine their activity and selectivity. On the basis of DFT calculations, we predict an enhanced reactivity of small planar clusters for reactions involving activation of the CC multiple bond in alkenes and alkynes by means of Lewis acid−base interactions, and a better catalytic performance of 3D gold nanoparticles in redox reactions involving bond dissociation by oxidative addition and new bond formation by reductive elimination. In the case of oxidation

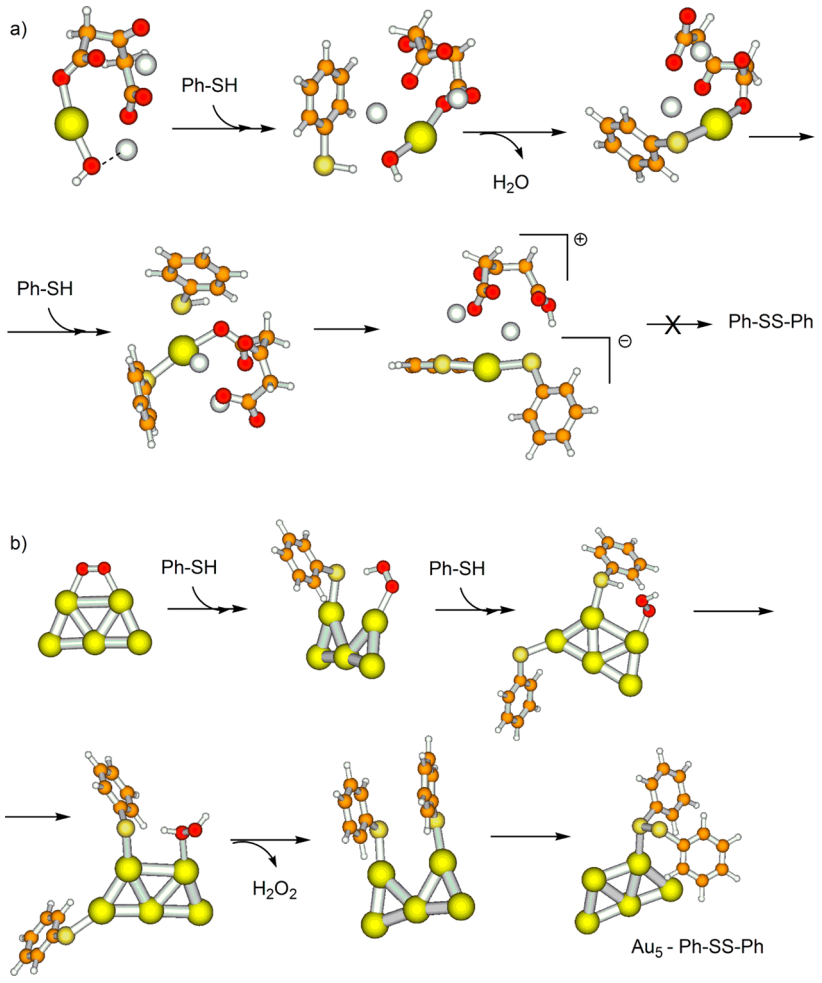

FIGURE 10. Structures involved in the mechanism of thiol oxidation catalyzed by (a) Au^I species and (b) Au_5 cluster. Au, S, C, O, and H atoms are depicted in gold, yellow, orange, red, and white, respectively.

reactions with molecular O_2, it is proposed that those processes requiring initial dissociation of O_2 into basic adsorbed oxygen atoms are more effectively catalyzed by gold nanoparticles of ~1 nm diameter, while small planar clusters should be more active for reactions following radical pathways involving peroxo or hydroperoxo intermediates. These predictions have been experimentally confirmed by testing the catalytic performance of gold nanoparticles and of small gold clusters stabilized on dendrimers or generated in situ in solution for several types of reactions.

Financial support from the Spanish Science and Innovation Ministry (Consolider Ingenio 2010-MULTICAT CSD2009-00050, Subprograma de apoyo a Centros y Universidades de Excelencia Severo Ochoa SEV 2012 0267, MAT2011-28009 projects) is acknowledged. A.L.-P. thanks ITQ for a contract.

BIOGRAPHICAL INFORMATION

Mercedes Boronat was born in Valencia in 1969 and obtained her Ph.D. from University of Valencia in 1999. She joined the Institute of Chemical Technology (ITQ) with a postdoctoral grant (1999−2001) and worked as a Junior Researcher in CEAM Foundation (2001−2003). Since 2007, she is a Tenured Scientist of the Spanish National Research Council (CSIC) at ITQ. Her work focuses on the theoretical study of reaction mechanisms, mostly heterogeneous catalyzed reactions over acid zeolites, metal nanoparticles, and metal oxides.

Antonio Leyva-Pérez was born in Sevilla in 1974 and studied Chemistry at the Universidad de Valencia (1994−2000). He received his Ph.D. by the Universidad Politécnica de Valencia in 2005 under the guidance of Prof. H. García. After stays at M.I.T. with Prof. S. L. Buchwald and at the University of Cambridge with Prof. S. V. Ley (postdoctoral), he joined the Instituto de Tecnología Química to work with Prof. A. Corma in the field of catalysis in organic synthesis.

Avelino Corma was born in Moncofa in 1951. He studied Chemistry at the Universidad de Valencia (1967−1973) and received his Ph.D. at the Universidad Complutense de Madrid in 1976. He was Postdoctoral in the Department of chemical engineering at the Queen's University (Canada, 1977−1979). He is Research Professor at the Instituto de Tecnología Química (UPV-CSIC) at the Universidad Politécnica de Valencia. His current research field is catalysis, covering aspects of synthesis, characterization, and reactivity in acid−base and redox catalysis. Avelino Corma is coauthor of more than 900 articles and 100 patents on these subjects.

FOOTNOTES

*To whom correspondence should be addressed. E-mail: acorma@itq.upv.es.
The authors declare no competing financial interest.

REFERENCES

1 Hashmi, A. S. K.; Hutchings, G. J. Gold catalysis. *Angew. Chem., Int. Ed.* **2006**, *45*, 7896–7936.
2 Corma, A.; Serna, P. Chemoselective hydrogenation of nitro compounds with supported gold catalysts. *Science* **2006**, *313*, 332–334.
3 Corma, A.; Garcia, H. Supported gold nanoparticles as catalysts for organic reactions. *Chem. Soc. Rev.* **2008**, *37*, 2096–2126.
4 Grirrane, A.; Corma, A.; Garcia, H. Gold-catalyzed synthesis of aromatic azo compounds from anilines and nitroaromatics. *Science* **2008**, *322*, 1661–1664.
5 Haruta, M. Size- and support-dependency in the catalysis of gold. *Catal. Today* **1997**, *36*, 153–166.
6 López, N.; Janssens, T. V. J.; Clausen, B. S.; Xu, Y.; Mavrikakis, M.; Bligaard, T.; Nørskov, J. K. On the origin of the catalytic activity of gold nanoparticles for low-temperature CO oxidation. *J. Catal.* **2004**, *223*, 232–235.
7 Haruta, M.; Tsubota, S.; Kobayashi, T.; Kageyama, H.; Genet, M. J.; Delmon, B. Low-temperature oxidation of CO over gold supported on TiO_2, α-Fe_2O_3, and Co_3O_4. *J. Catal.* **1993**, *144*, 175–192.
8 Abad, A.; Corma, A.; García, H. Catalyst parameters determining activity and selectivity of supported gold nanoparticles for the aerobic oxidation of alcohols: the molecular reaction mechanism. *Chem.—Eur. J.* **2008**, *14*, 212–222.
9 Tsunoyama, H.; Ichikuni, N.; Sakurai, H.; Tsukuda, T. Effect of electronic structures of Au clusters stabilized by poly(N-vinyl-2-pyrrolidone) on aerobic oxidation catalysis. *J. Am. Chem. Soc.* **2009**, *131*, 7086–7093.
10 Chen, M. S.; Goodman, D. W. Catalytically active gold: from nanoparticles to ultrathin films. *Acc. Chem. Res.* **2006**, *39*, 739–746.
11 Boronat, M.; Corma, A.; Illas, F.; Radilla, J.; Ródenas, T.; Sabater, M. J. Mechanism of selective alcohol oxidation to aldehydes on gold catalysts: Influence of surface roughness on reactivity. *J. Catal.* **2011**, *278*, 50–58.
12 Hayashi, T.; Tanaka, K.; Haruta, M. Selective vapor-phase epoxidation of propylene over Au/TiO_2 catalysts in the presence of oxygen and hydrogen. *J. Catal.* **1998**, *178*, 566–575.
13 Huang, J.; Lima, E.; Akita, T.; Guzman, A.; Qi, C.; Takei, T.; Haruta, M. Propene epoxidation with O_2 and H_2: identification of the most active gold clusters. *J. Catal.* **2011**, *278*, 8–15.
14 Lee, W. S.; Zhang, R.; Akatay, M. C.; Baertsch, C. D.; Stach, E. A.; Ribeiro, F. H.; Delgass, W. N. Differences in catalytic sites for CO oxidation and propylene epoxidation on Au nanoparticles. *ACS Catal.* **2011**, *1*, 1327–1330.
15 Liu, Y.; Tsunoyama, H.; Akita, T.; Xie, S.; Tsukuda, T. Aerobic oxidation of cyclohexane catalyzed by size-controlled Au clusters on hydroxyapatite: size effect in the sub-2 nm regime. *ACS Catal.* **2011**, *1*, 2–6.
16 Lu, J.; Aydin, C.; Browning, N. D.; Gates, B. C. Imaging Isolated Gold Atom Catalytic Sites in Zeolite NaY. *Angew. Chem., Int. Ed.* **2012**, *51*, 5842–5846.
17 Herzing, A. A.; Kiely, C. J.; Carley, A. F.; Landon, P.; Hutchings, G. J. Identification of active gold nanoclusters on iron oxide supports for CO oxidation. *Science* **2008**, *321*, 1331–1332.
18 Lee, S.; Molina, L. M.; López, M. J.; Alonso, J. A.; Hammer, B.; Lee, B.; Seifert, S.; Winans, R. E.; Elam, J. W.; Pellin, M. J.; Vajda, S. Selective propene epoxidation on immobilized Au_{6-10} clusters: the effect of hydrogen and water on activity and selectivity. *Angew. Chem., Int. Ed.* **2009**, *48*, 1467–1471.
19 Robinson, P. S. D.; Khairallah, G. N.; da Silva, G.; Lioe, H.; O'Hair, R. A. J. Gold-mediated C—I bond activation of iodobenzene. *Angew. Chem., Int. Ed.* **2012**, *51*, 3812–3817.
20 Kyriakou, G.; Beaumont, S. K.; Humphrey, S. M.; Antonetti, C.; Lambert, R. M. Sonogashira coupling catalyzed by gold nanoparticles: does homogeneous or heterogeneous catalysis dominate? *ChemCatChem* **2010**, *2*, 1444–1449.
21 Corma, A.; Juarez, R.; Boronat, M.; Sánchez, F.; Iglesias, M.; Garcia, H. Gold catalyzes the Sonogashira coupling reaction without the requirement of palladium impurities. *Chem. Commun.* **2011**, *47*, 1446–1448.
22 Boronat, M.; Combita, D.; Concepción, P.; Corma, A.; García, H.; Juárez, R.; Laursen, S.; López-Castro, J. de D. Making C-C bonds with gold: identification of selective gold sites for homo- and cross-coupling reactions between iodobenzene and alkynes. *J. Phys. Chem. C* **2012**, *116*, 24855–24867.
23 Häkkinen, H.; Yoon, B.; Landman, U.; Li, X.; Zhai, H.-J.; Wang, L.-S. On the Electronic and Atomic Structures of Small Au_N^- (N = 4−14) Clusters: A Photoelectron Spectroscopy and Density-Functional Study. *J. Phys. Chem. A* **2003**, *107*, 6168–6175.
24 Häkkinen, H. Atomic and electronic structure of gold clusters: understanding flakes, cages and superatoms from simple concepts. *Chem. Soc. Rev.* **2008**, *37*, 1847–1859.
25 Carrettin, S.; Guzman, J.; Corma, A. Supported Gold Catalyzes the Homocoupling of Phenylboronic Acid with High Conversion and Selectivity. *Angew. Chem., Int. Ed.* **2005**, *44*, 2242–2245.
26 Gonzalez-Arellano, C.; Abad, A.; Corma, A.; Garcia, H.; Iglesias, M.; Sanchez, F. Catalysis by Gold(I) and Gold(III): A Parallelism between Homo- and Heterogeneous Catalysts for Copper-Free Sonogashira Cross-Coupling Reactions. *Angew. Chem., Int. Ed.* **2007**, *46*, 1536–1538.
27 Han, J.; Liu, Y.; Guo, R. Facile synthesis of highly stable gold nanoparticles and their unexpected excellent catalytic activity for Suzuki−Miyaura cross-coupling reaction in water. *J. Am. Chem. Soc.* **2009**, *131*, 2060–2061.

28 Mills, G.; Gordon, M. S.; Metiu, H. Oxygen adsorption on Au clusters and a rough Au(111) surface: The role of surface flatness, electron confinement, excess electrons, and band gap. *J. Chem. Phys.* **2003**, *118*, 4198–4205.

29 Boronat, M.; Corma, A. Oxygen activation on gold nanoparticles: separating the influence of particle size, particle shape and support interaction. *Dalton Trans.* **2010**, *39*, 8538–8546.

30 Pal, R.; Wang, L.-M.; Pei, Y.; Wang, L.-S.; Zeng, X. C. Unraveling the mechanisms of O_2 activation by size-selected gold clusters: transition from superoxo to peroxo chemisorption. *J. Am. Chem. Soc.* **2012**, *134*, 9438–9445.

31 Yoon, B.; Häkkinen, H.; Landman, U. Interaction of O_2 with gold clusters: molecular and dissociative adsorption. *J. Phys. Chem. A* **2003**, *107*, 4066–4071.

32 Alves, L.; Ballesteros, B.; Boronat, M.; Cabrero-Antonino, J. R.; Concepción, P.; Corma, A.; Correa-Duarte, M. A.; Mendoza, E. *J. Am. Chem. Soc.* **2011**, *133*, 10251–10261.

33 Baker, T. A.; Xu, B.; Liu, X.; Kaxiras, E.; Friend, C. M. *J. Phys. Chem. C* **2009**, *113*, 16561–16564.

34 Pulido, A.; Boronat, M.; Corma, A. Propene epoxidation with $H_2/H_2O/O_2$ mixtures over gold atoms supported on defective graphene: a theoretical study. *J. Phys. Chem. C* **2012**, *116*, 19355–19362.

35 Oliver-Meseguer, J.; Cabrero-Antonino, J. R.; Dominguez, I.; Leyva-Perez, A.; Corma, A. Small gold clusters formed in solution give reaction turnover numbers of 10^7 at room temperature. *Science* **2012**, *338*, 1452–1455.

36 Zheng, J.; Zhang, C.; Dickson, R. M. Highly Fluorescent,Water-Soluble, Size-Tunable Gold Quantum Dots. *Phys. Rev. Lett.* **2004**, *93* (7), 077402-1–077402-4.

37 Mo, F.; Yan, J. M.; Qiu, D.; Li, F.; Zhang, Y.; Wang, J. Gold-catalyzed halogenation of aromatics by N-halosuccinimides. *Angew. Chem., Int. Ed.* **2010**, *49*, 2028–2032.

38 Kanuru, V. K.; Kyriakou, G.; Beaumont, S. K.; Papageorgiou, A. C.; Watson, D. J.; Lambert, R. M. Sonogashira coupling on an extended gold surface in vacuo: reaction of phenylacetylene with iodobenzene on Au(111). *J. Am. Chem. Soc.* **2010**, *132*, 8081–8086.

39 Guan, Y.; Hensen, E. J. M. Ethanol dehydrogenation by gold catalysts: The effect of the gold particle size and the presence of oxygen. *Appl. Catal. A: Gen.* **2009**, *361*, 49–56.

40 Comotti, M.; Della Pina, C.; Matarrese, R.; Rossi, M. The Catalytic Activity of "Naked" Gold Particles. *Angew. Chem., Int. Ed.* **2004**, *43*, 5812–5815.

41 Kanaoka, S.; Yagi, N.; Fukuyama, Y.; Aoshima, S.; Tsunoyama, H.; Tsukuda, T.; Sakurai, H. Thermosensitive Gold Nanoclusters Stabilized by Well-Defined Vinyl Ether Star Polymers: Reusable and Durable Catalysts for Aerobic Alcohol Oxidation. *J. Am. Chem. Soc.* **2007**, *129*, 12060–12061.

42 Boronat, M.; Corma, A. Molecular approaches to catalysis. Naked gold nanoparticles as quasi-molecular catalysts for green processes. *J. Catal.* **2011**, *284*, 138–147.

43 Corma, A.; Rodenas, T.; Sabater, M. J. Aerobic oxidation of thiols to disulfides by heterogeneous gold catalysts. *Chem. Sci.* **2012**, *3*, 398–404.

44 Concepción, P.; Boronat, M.; Sabater, M. J.; Navas, J.; Yacaman, M. J.; Larios, E.; Posadas, A.; López-Quintela, M. A.; Buceta, D.; Mendoza, E.; Mayoral, A.; Guilera, G.; Corma, A. Reaching enzyme activities with size controlled supported gold clusters of low atomicity. Submitted to Nature Chemistry.

45 Jadzinsky, P. D.; Calero, G.; Ackerson, C. J.; Bushnell, D. A.; Kornberg, R. D. Structure of a thiol monolayer-protected gold nanoparticle at 1.1Å resolution. *Science* **2007**, *318*, 430–433.

46 Häkkinen, H. The gold-sulfur interface at the nanoscale. *Nat. Chem.* **2012**, *4*, 443–455.